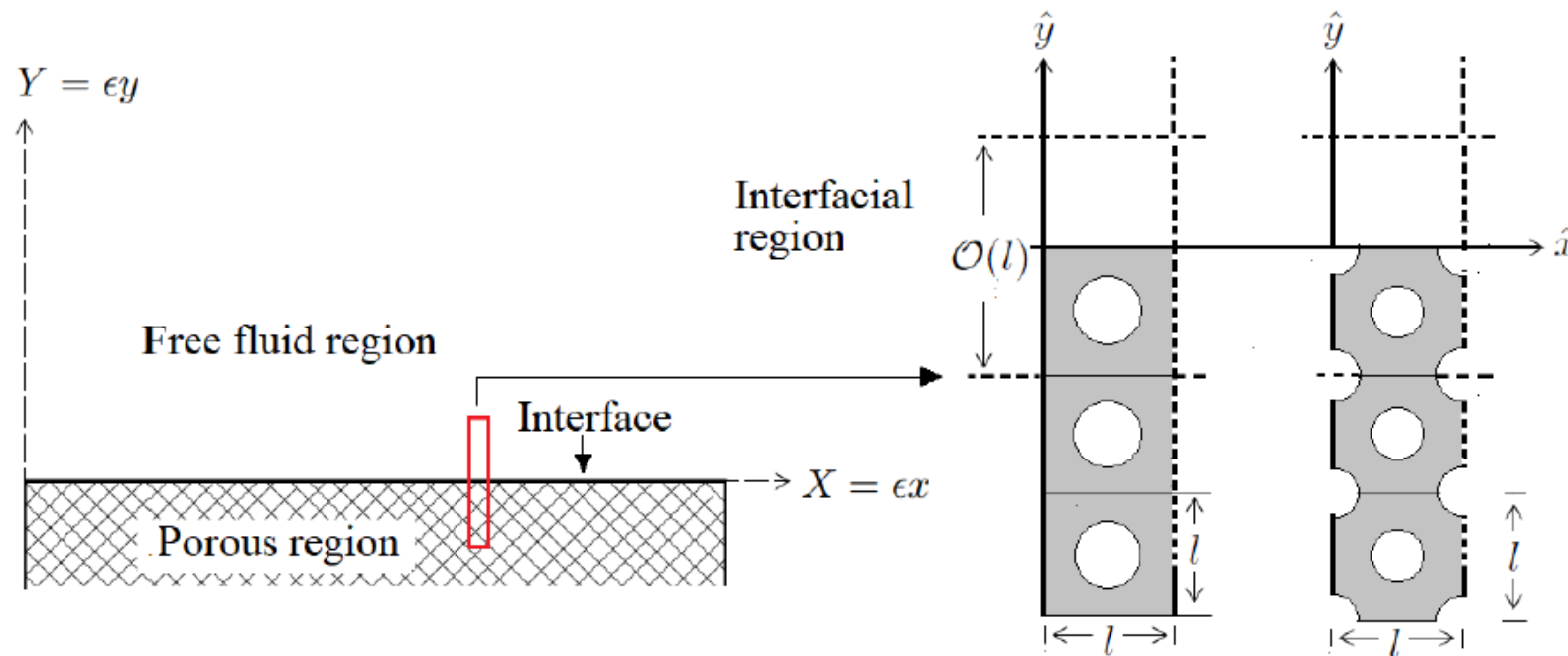




# Interfacial conditions between a free-fluid region and a porous medium: revisiting Beavers & Joseph



Based on joint work with Sahrish B. Naqvi.

## Beavers and Joseph (1967)

Classical experimental work on interface condition between free-fluid and porous domain

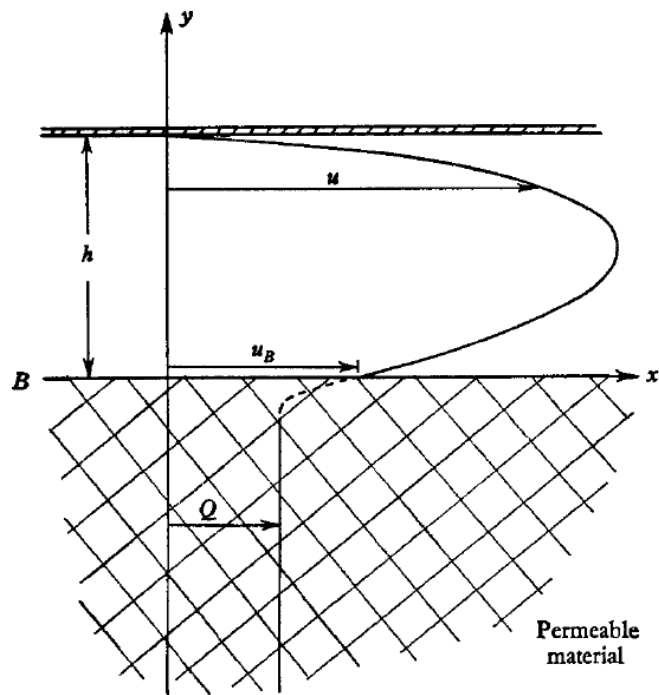


FIGURE 1. Velocity profile for the rectilinear flow in a horizontal channel formed by a permeable lower wall ( $y = 0$ ) and an impermeable upper wall ( $y = h$ ).

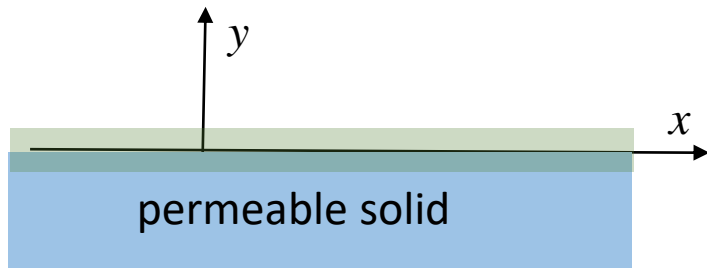
$$\frac{du}{dy} \Big|_{y=0_+} = \frac{\alpha}{\sqrt{k}} (u_B - Q) \quad Q = -\frac{k}{\mu} \frac{dP}{dx}$$

with  $\alpha$  a dimensionless function of the structural properties of the porous matrix

Block	$k(\text{in.}^2)$	$\alpha$	Average pore size (in.)
Foametal A	$1.5 \times 10^{-5}$	0.78	0.016
Foametal B	$6.1 \times 10^{-5}$	1.45	0.034
Foametal C	$12.7 \times 10^{-5}$	4.0	0.045
Aloxite	$1.0 \times 10^{-6}$	0.1	0.013
Aloxite	$2.48 \times 10^{-6}$	0.1	0.027



## Saffman (1971)



$$-\mu \nabla^2 \mathbf{u} + \nabla p = 0, \quad \text{for } y > 0$$

$$\mu \frac{\mathbf{U}^{(0)}}{k} + \nabla \bar{p} = 0, \quad \text{for } y < 0$$

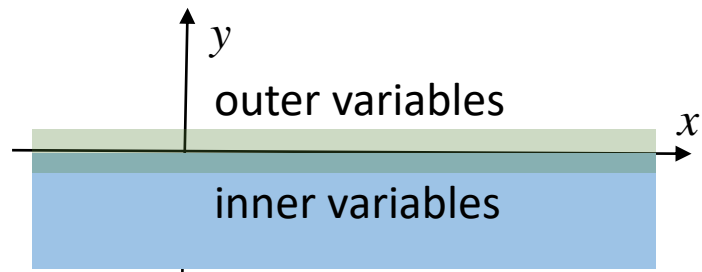
The velocity  $\mathbf{U}$  in the *intermediate/boundary layer* must satisfy asymptotic matching conditions:

$$\lim_{y/k^{1/2} \rightarrow \infty} \mathbf{U} = \lim_{y \rightarrow 0^+} \mathbf{u},$$

$$\lim_{y/k^{1/2} \rightarrow -\infty} \mathbf{U} = \lim_{y \rightarrow 0^-} \mathbf{U}^{(0)},$$



## Saffman (1971)

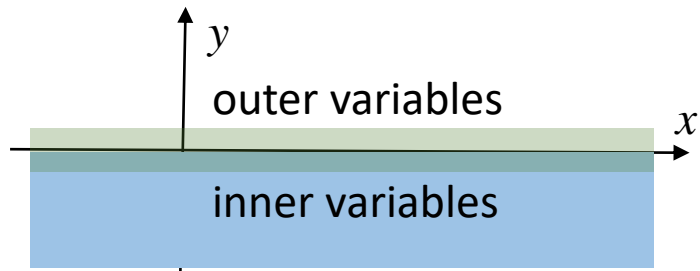


Using linearity and expanding intermediate layer variables in terms of delta function derivatives, Saffman finds the asymptotic expressions of the velocity in the outer layer as  $y \rightarrow 0^+$ :

$$u = \frac{k^{1/2}}{\alpha} \frac{\partial u}{\partial y} + O(k) \quad \text{on } y = 0.$$



## Saffman (1971)



Using linearity and expanding intermediate layer variables in terms of delta function derivatives, Saffman finds the asymptotic expressions of the velocity in the outer layer as  $y \rightarrow 0^+$ :

$$u = \frac{k^{1/2}}{\alpha} \frac{\partial u}{\partial y} + O(k) \quad \text{on } y = 0.$$

The result by Saffman permits to find the outer flow solution without iterating between inner and outer domains. Elaborating upon Saffman's results it is possible to find the order  $k$  correction:

$$\hat{u} = -\frac{Bk}{\mu} \frac{\partial \hat{p}^-}{\partial \hat{x}} + \hat{\lambda} \frac{\partial \hat{u}}{\partial \hat{y}} \quad \text{on } y = 0.$$



## Wall slip

Henri Navier, 1823



(the smooth wall)

Si elle était perpendiculaire à l'axe des  $y$ ,

$$Eu + \varepsilon \frac{du}{dy} = 0, \quad Ew + \varepsilon \frac{dw}{dy} = 0;$$

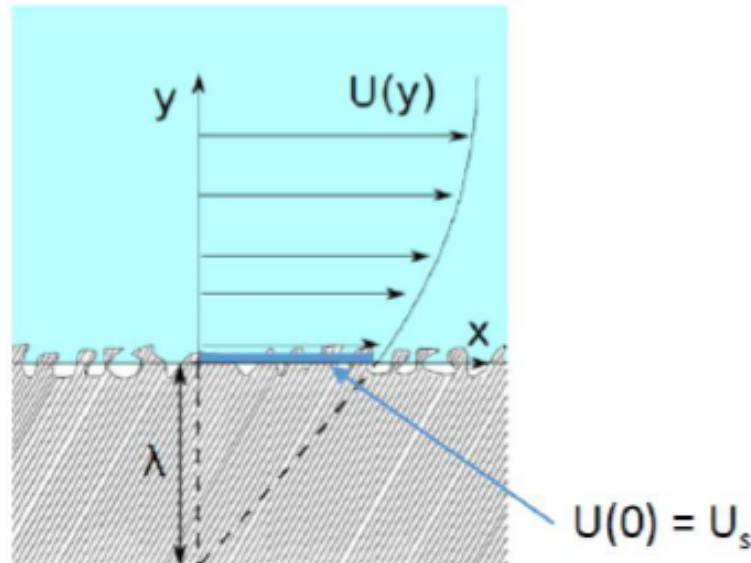
La valeur de la constante  $E$  doit varier suivant la nature des corps avec lesquels le fluide est en contact, et ( ce qui est physiquement impossible ) s'il y avait un espace vide au-dessus de la portion libre de la surface du fluide, ces équations devraient encore être satisfaites pour les points appartenant à cette portion, en  $y$  supposant  $\bar{E} = 0$ .

.... la constante  $\varepsilon$  représente en unités de poids la résistance provenant du glissement de deux couches quelconques l'une sur l'autre, pour une étendue égale à l'unité superficielle.



In today's words and terminology, Navier's argument was that there is *partial slip*, and the resistance of the wall is proportional to the slip velocity  $U_s$ :

$$E U_s = -\varepsilon \left. \frac{dU}{dy} \right|_{y=0} \rightarrow U(0) = (-\varepsilon/E) \left. \frac{dU}{dy} \right|_{y=0} = \lambda \left. \frac{dU}{dy} \right|_{y=0}$$



$\lambda$  = slip length



- Navier's slip condition is a first-order development around a fictitious wall (the position  $y = 0$  is arbitrary) applicable when either
  - (i) the surface geometry is microstructured or
  - (ii) the continuum approximation breaks down.
- There is a unique slip length  $\lambda$  for  $U$  and  $W$  only for isotropic (in  $x, z$ ) walls. The general (anisotropic) case requires (to first order) that:

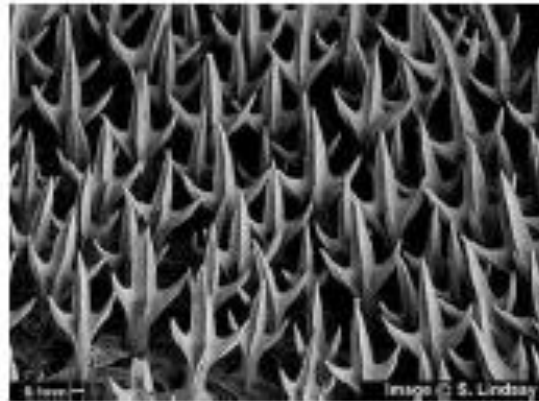
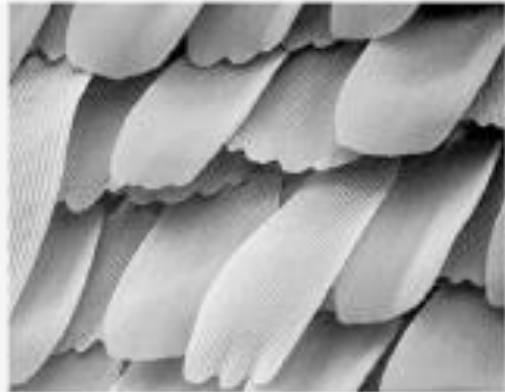
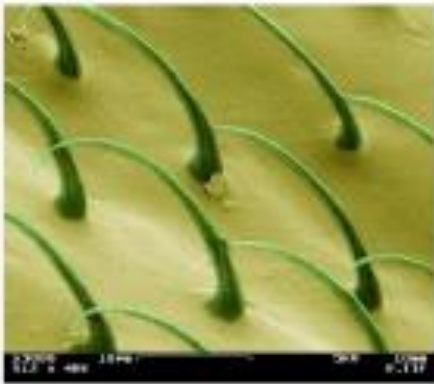
$$\begin{bmatrix} U(x, 0, z) \\ W(x, 0, z) \end{bmatrix} = \Lambda \frac{\partial}{\partial y} \begin{bmatrix} U(x, 0, z) \\ W(x, 0, z) \end{bmatrix},$$

with  $\Lambda$  a slip tensor (plus a *non-penetration* condition for  $V$ ).





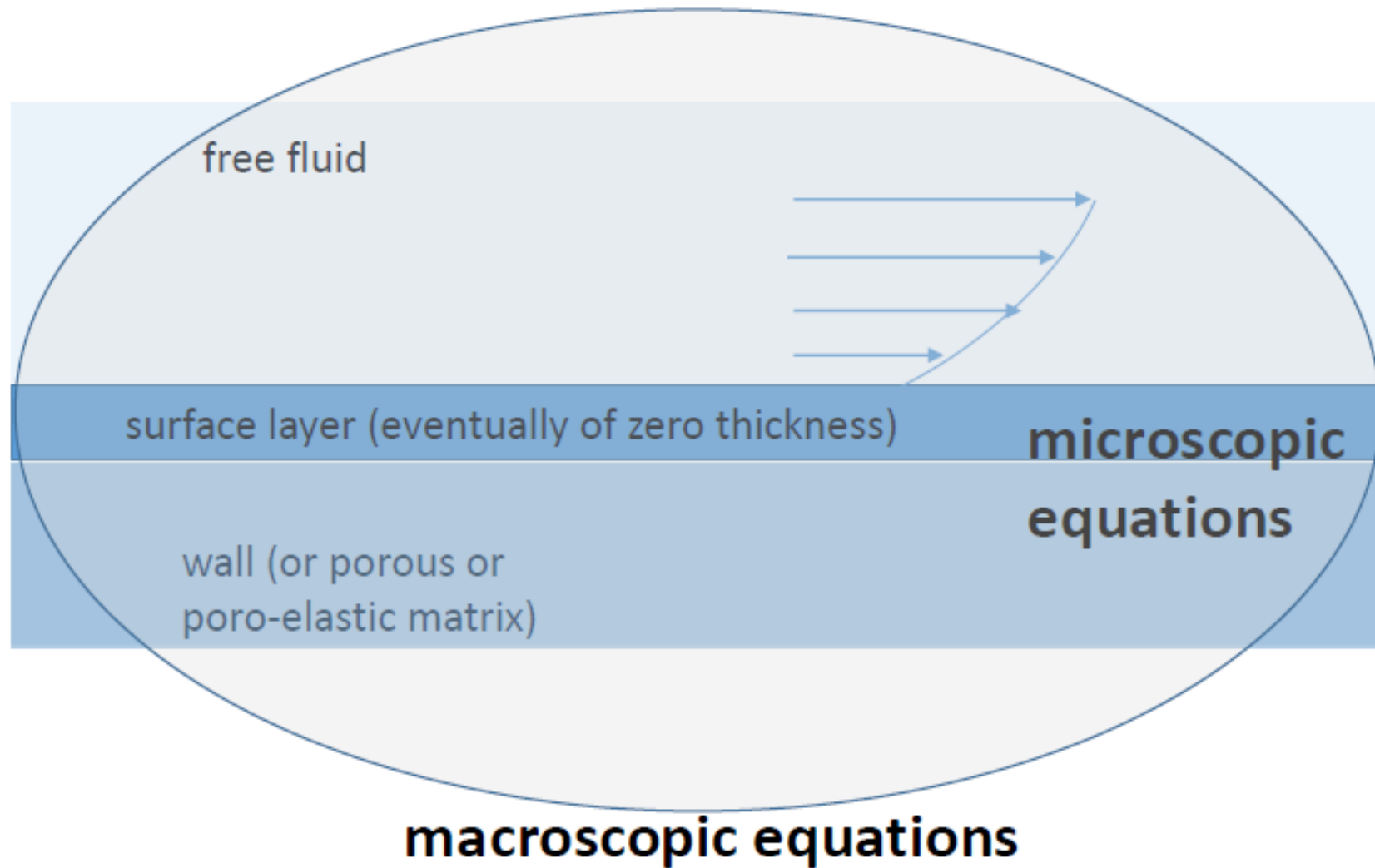
Biomimetics: irregular surfaces, possibly with regularly micro-structured porous substrates, are the norm, not the exception



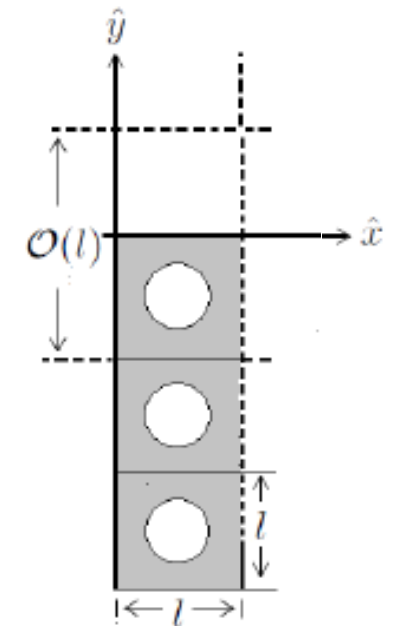


Our approach to the dividing surface conditions:

Asymptotic homogenization/multiple scales, under the simplifying hypothesis that the porous medium is formed by a regular array of isotropic solid grains



*unit cell*





$\hat{y}$

## SCALES

$$(\epsilon = l/L)$$

outer flow  
region (+)

$$L, L/\mathcal{U}, \mathcal{U}, \text{ and } \rho\mathcal{U}^2$$

intermediate/surface  
region (=)

$$l = \epsilon L, L/\mathcal{U}, \epsilon\mathcal{U}, \text{ and } \mu\mathcal{U}/L$$

inner flow  
region (-)

$$l = \epsilon L, \epsilon^2\mathcal{U}, \text{ and } \mu\mathcal{U}/L$$



$\hat{y}$

## EQUATIONS

outer flow  
region  $\oplus$

$$\frac{\partial U_i^+}{\partial X_i} = 0, \quad \frac{\partial U_i^+}{\partial t} + U_j^+ \frac{\partial U_i^+}{\partial X_j} = -\frac{\partial P^+}{\partial X_i} + \frac{1}{Re} \frac{\partial^2 U_i^+}{\partial X_j^2}$$

$$Re = \rho U L / \mu$$

intermediate  
region  $\ominus$

$$\frac{\partial U_i^-}{\partial x_i} = 0, \quad \epsilon^2 Re \left( \frac{\partial U_i^-}{\partial t} + U_j^- \frac{\partial U_i^-}{\partial x_j} \right) = -\frac{\partial P^-}{\partial x_i} + \frac{\partial^2 U_i^-}{\partial x_j^2}$$

inner flow  
region  $\ominus$

$$\epsilon \frac{\partial U_i^-}{\partial x_i} = 0, \quad \epsilon^4 Re U_j^- \frac{\partial U_i^-}{\partial x_j} = -\frac{\partial P^-}{\partial x_i} + \epsilon \frac{\partial^2 U_i^-}{\partial x_j^2}$$



$$y = Y/\epsilon$$

outer flow  
region  $(+)$

$$\lim_{y \rightarrow +\infty} (U^-, V^-) = \frac{1}{\epsilon} \lim_{Y \rightarrow 0^+} (U^+, V^+)$$

intermediate  
region  $(=)$

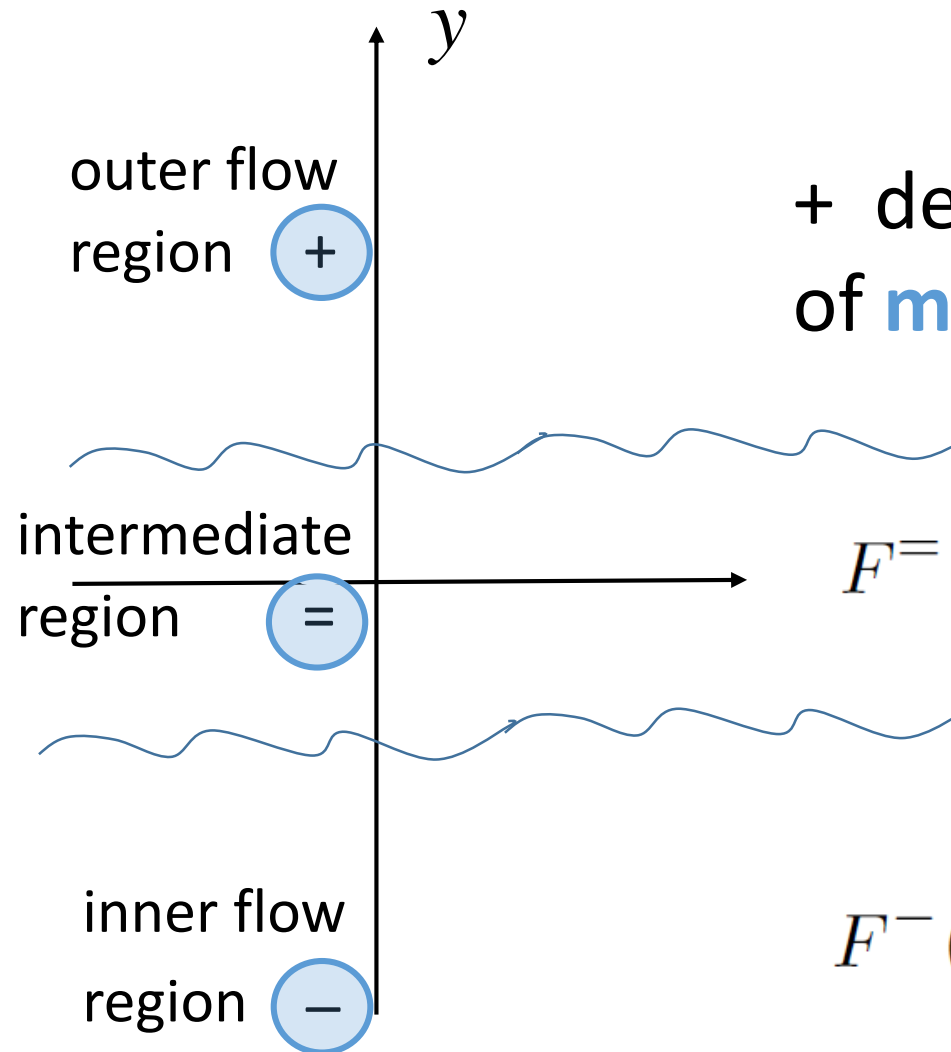
$$\lim_{y \rightarrow +\infty} \left( \frac{\partial U^-}{\partial y} + \frac{\partial V^-}{\partial x}, -P^- + 2 \frac{\partial V^-}{\partial y} \right) = \lim_{Y \rightarrow 0^+} \left( \frac{\partial U^+}{\partial Y} + \frac{\partial V^+}{\partial X}, -Re P^+ + 2 \frac{\partial V^+}{\partial Y} \right)$$

inner flow  
region  $(-)$

1-periodicity when  $y \rightarrow -\infty$  (i.e. in the Darcy region)



We now develop a *composite description* for the  $=$  and  $-$  regions, and enforce matching conditions at  $y \rightarrow \pm\infty$

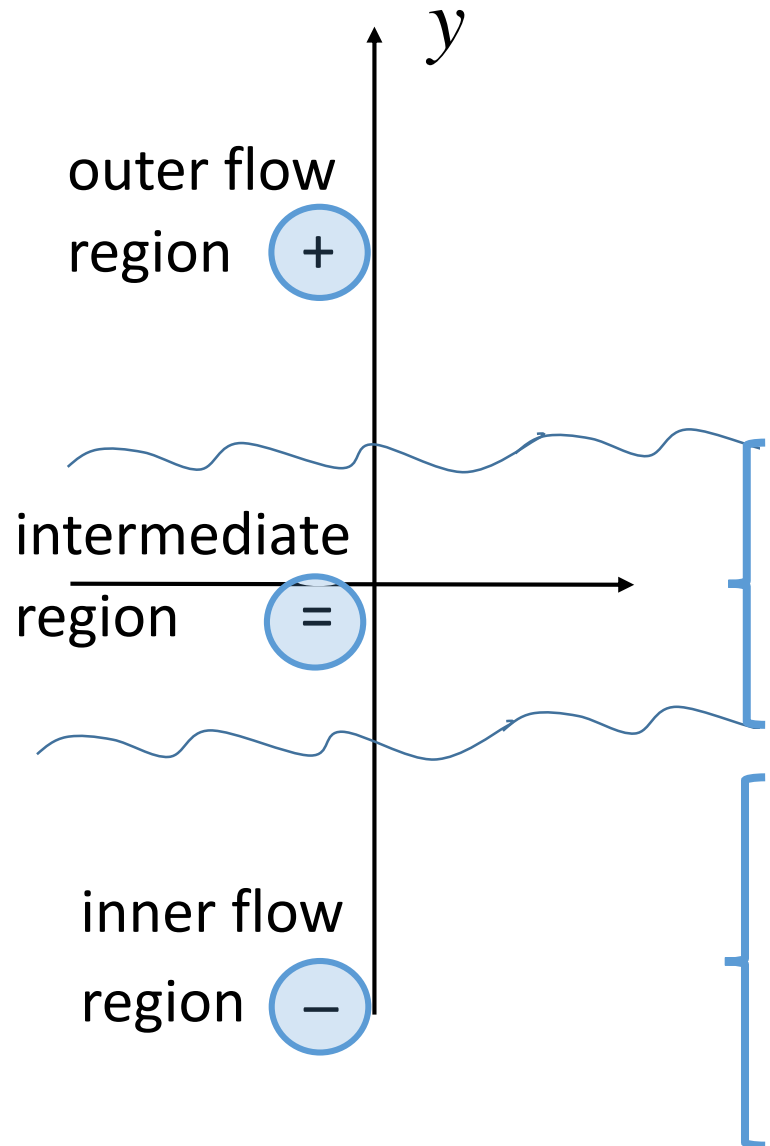


+ dependent variables: only function  
of **macroscopic** independent variables

$$F^{\bar{}}(x_i, X_i, t) = F_0^{\bar{}} + \epsilon F_1^{\bar{}} + \epsilon^2 F_2^{\bar{}} + \dots$$

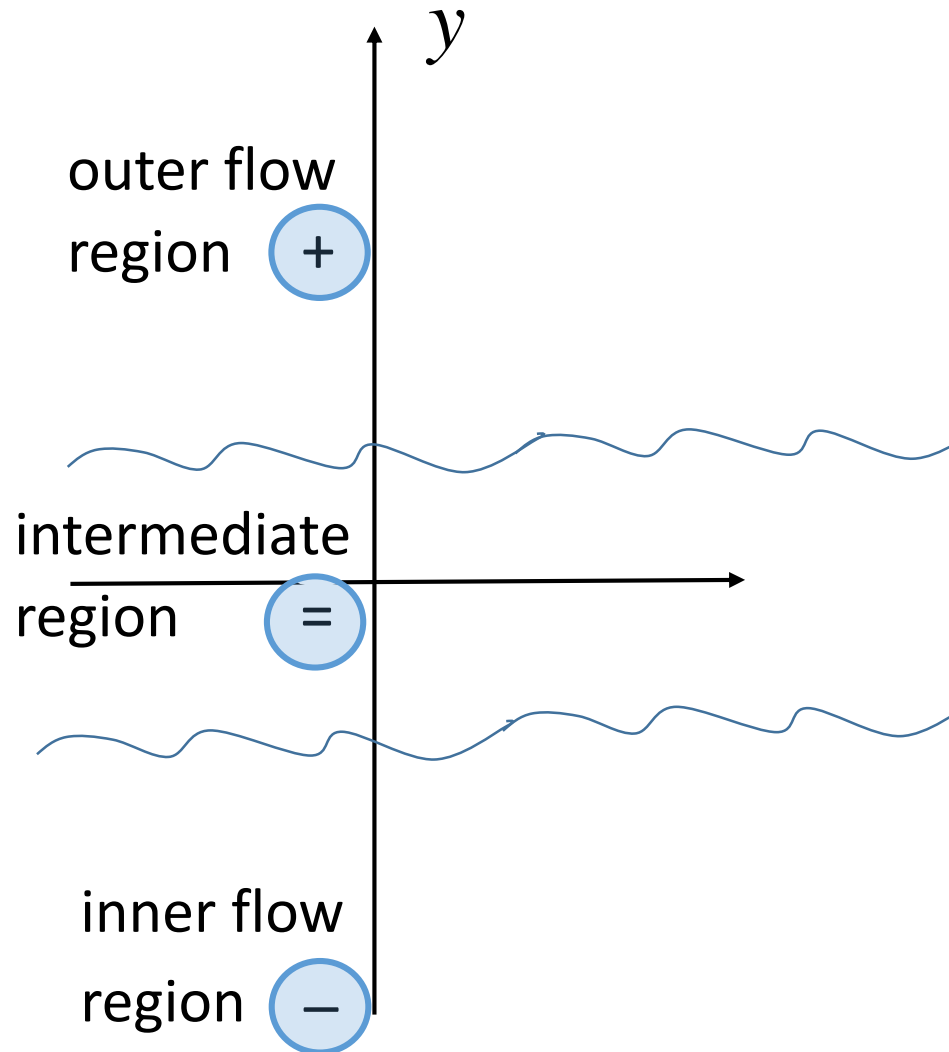
$$F^{\bar{}}(x_i, X_i, t) = F_0^{\bar{}} + \epsilon F_1^{\bar{}} + \epsilon^2 F_2^{\bar{}} + \dots$$





$$\frac{\partial}{\partial x_j} \rightarrow \frac{\partial}{\partial x_j} + \epsilon \frac{\partial}{\partial X_j}$$

$\mathcal{O}(\epsilon^0) :$	$\frac{\partial U_{i0}^-}{\partial x_i} = 0, \quad -\frac{\partial P_0^-}{\partial x_i} + \frac{\partial^2 U_{i0}^-}{\partial x_j^2} = 0,$
$\mathcal{O}(\epsilon^1) :$	$\frac{\partial U_{i1}^-}{\partial x_i} = -\frac{\partial U_{i0}^-}{\partial X_i}, \quad -\frac{\partial P_1^-}{\partial x_i} + \frac{\partial^2 U_{i1}^-}{\partial x_j^2} = \frac{\partial P_0^-}{\partial X_i} - 2 \frac{\partial^2 U_{i0}^-}{\partial x_j \partial X_j}.$
$\mathcal{O}(\epsilon^0) :$	$\frac{\partial P_0^-}{\partial x_i} = 0,$
$\mathcal{O}(\epsilon^1) :$	$\frac{\partial U_{i0}^-}{\partial x_i} = 0, \quad -\frac{\partial P_1^-}{\partial x_i} + \frac{\partial^2 U_{i0}^-}{\partial x_j^2} = \frac{\partial P_0^-}{\partial X_i},$
$\mathcal{O}(\epsilon^2) :$	$\frac{\partial U_{i1}^-}{\partial x_i} = -\frac{\partial U_{i0}^-}{\partial X_i}, \quad -\frac{\partial P_2^-}{\partial x_i} + \frac{\partial^2 U_{i1}^-}{\partial x_j^2} = \frac{\partial P_1^-}{\partial X_i} - 2 \frac{\partial^2 U_{i0}^-}{\partial x_j \partial X_j}.$



## COMPOSITE DESCRIPTION

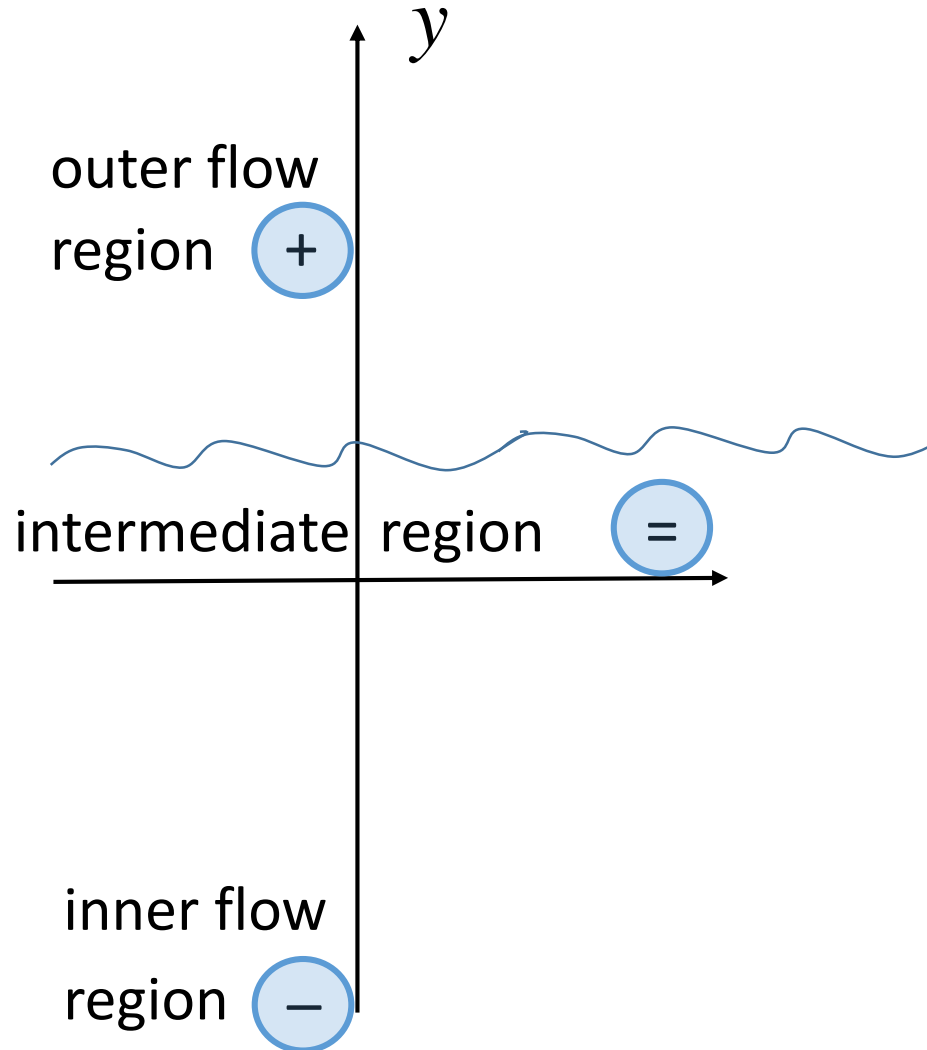
$$\begin{aligned}
 u_i &= u_i^{(0)} + \epsilon u_i^{(1)} + \mathcal{O}(\epsilon^2), \\
 p &= p^{(0)} + \epsilon p^{(1)} + \mathcal{O}(\epsilon^2),
 \end{aligned}$$

$$u_i^{(0)} = \begin{cases} U_{i0}^- & y > 0, \\ \epsilon U_{i0}^- & y < 0, \end{cases}$$

$$p^{(0)} = \begin{cases} P_0^- & y > 0, \\ P_0^- + \epsilon P_1^- & y < 0, \end{cases}$$

$$u_i^{(1)} = \begin{cases} U_{i1}^- & y > 0, \\ \epsilon U_{i1}^- & y < 0, \end{cases}$$

$$p^{(1)} = \begin{cases} P_1^- & y > 0, \\ \epsilon P_2^- & y < 0. \end{cases}$$



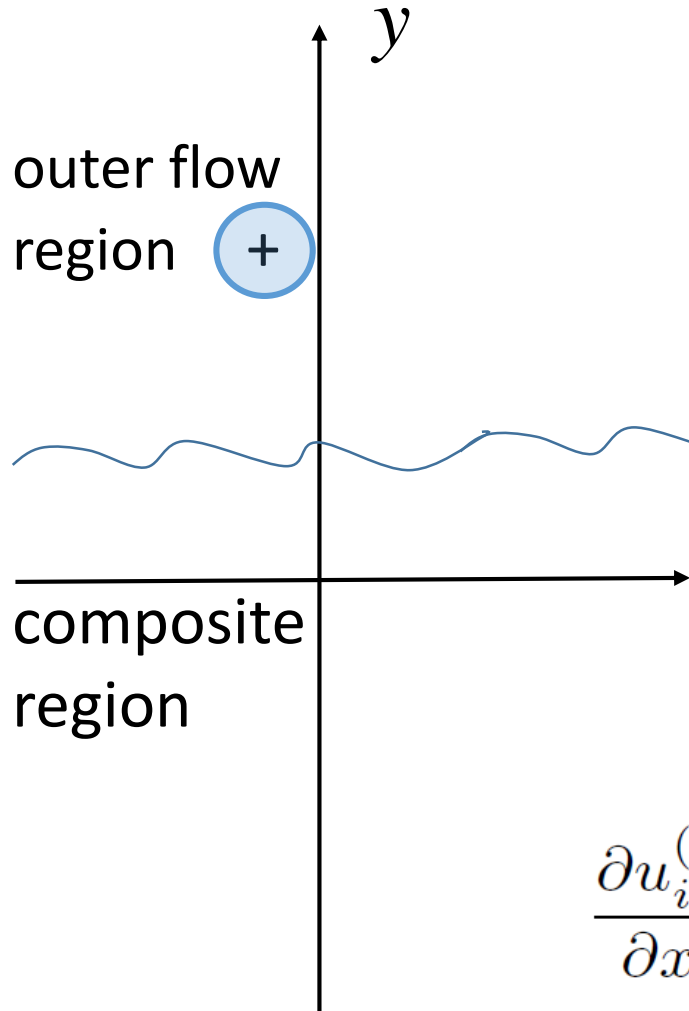
## “Two-domain” approach

$$u_i^{(0)} = \begin{cases} U_{i0}^- & y > 0, \\ \epsilon U_{i0}^- & y < 0, \end{cases}$$

$$p^{(0)} = \begin{cases} P_0^- & y > 0, \\ P_0^- + \epsilon P_1^- & y < 0, \end{cases}$$

$$u_i^{(1)} = \begin{cases} U_{i1}^- & y > 0, \\ \epsilon U_{i1}^- & y < 0, \end{cases}$$

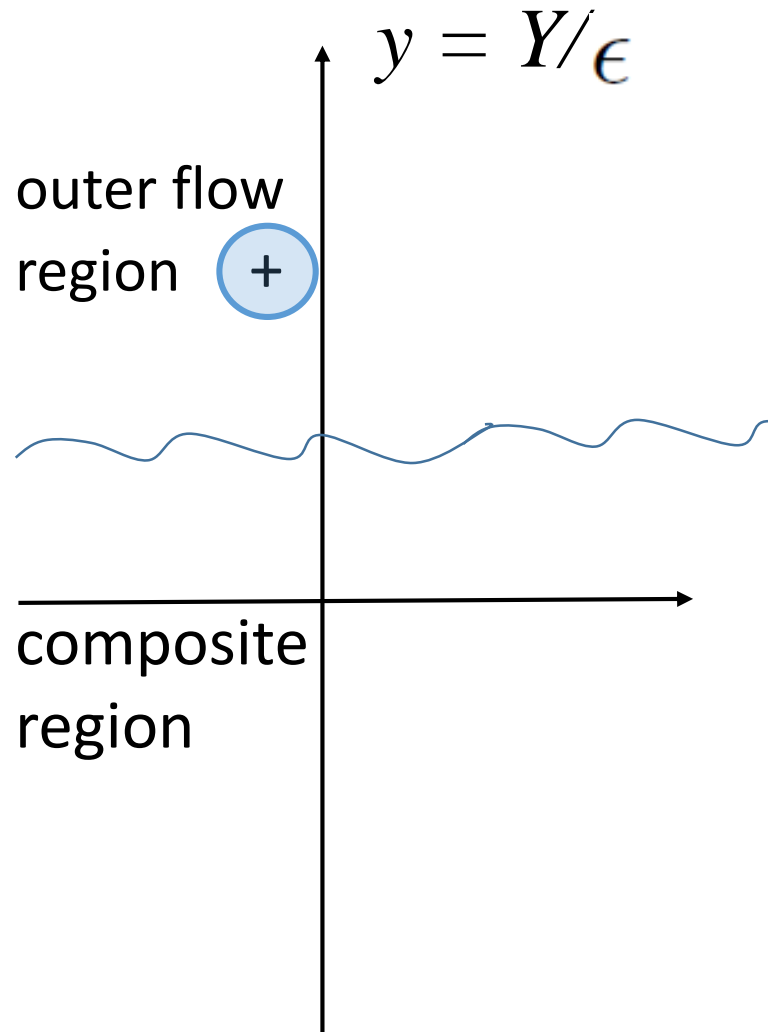
$$p^{(1)} = \begin{cases} P_1^- & y > 0, \\ \epsilon P_2^- & y < 0. \end{cases}$$



**COMPOSITE DESCRIPTION**  
for = and - regions  
(valid up to first order in  $\epsilon$ )

$$\frac{\partial u_i^{(0)}}{\partial x_i} = 0, \quad -\frac{\partial p^{(0)}}{\partial x_i} + \frac{\partial^2 u_i^{(0)}}{\partial x_j^2} = 0,$$

$$\frac{\partial u_i^{(1)}}{\partial x_i} = -\frac{\partial u_i^{(0)}}{\partial X_i} - \frac{\partial p^{(1)}}{\partial x_i} + \frac{\partial^2 u_i^{(1)}}{\partial x_j^2} = \frac{\partial p^{(0)}}{\partial X_i} - 2 \frac{\partial^2 u_i^{(0)}}{\partial x_j \partial X_j}.$$

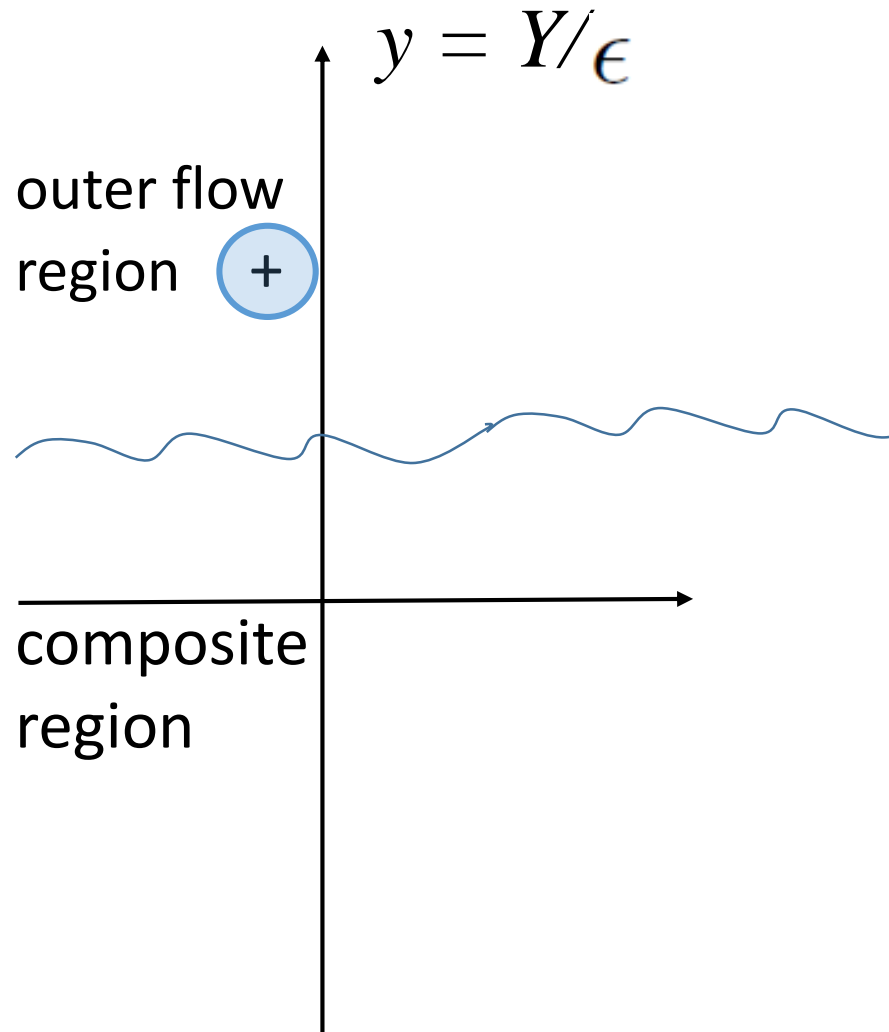


## BOUNDARY CONDITIONS

$$\lim_{y \rightarrow +\infty} (u, v) = \frac{1}{\epsilon} \lim_{Y \rightarrow 0^+} (U, V),$$

$$\lim_{y \rightarrow +\infty} \left( \frac{\partial u}{\partial y} + \frac{\partial v}{\partial x}, -p + 2 \frac{\partial v}{\partial y} \right) = \lim_{Y \rightarrow 0^+} \left( \frac{\partial U}{\partial Y} + \frac{\partial V}{\partial X}, -Re P + 2 \frac{\partial V}{\partial Y} \right).$$

1-periodicity when  $y \rightarrow -\infty$  (i.e. in the Darcy region)

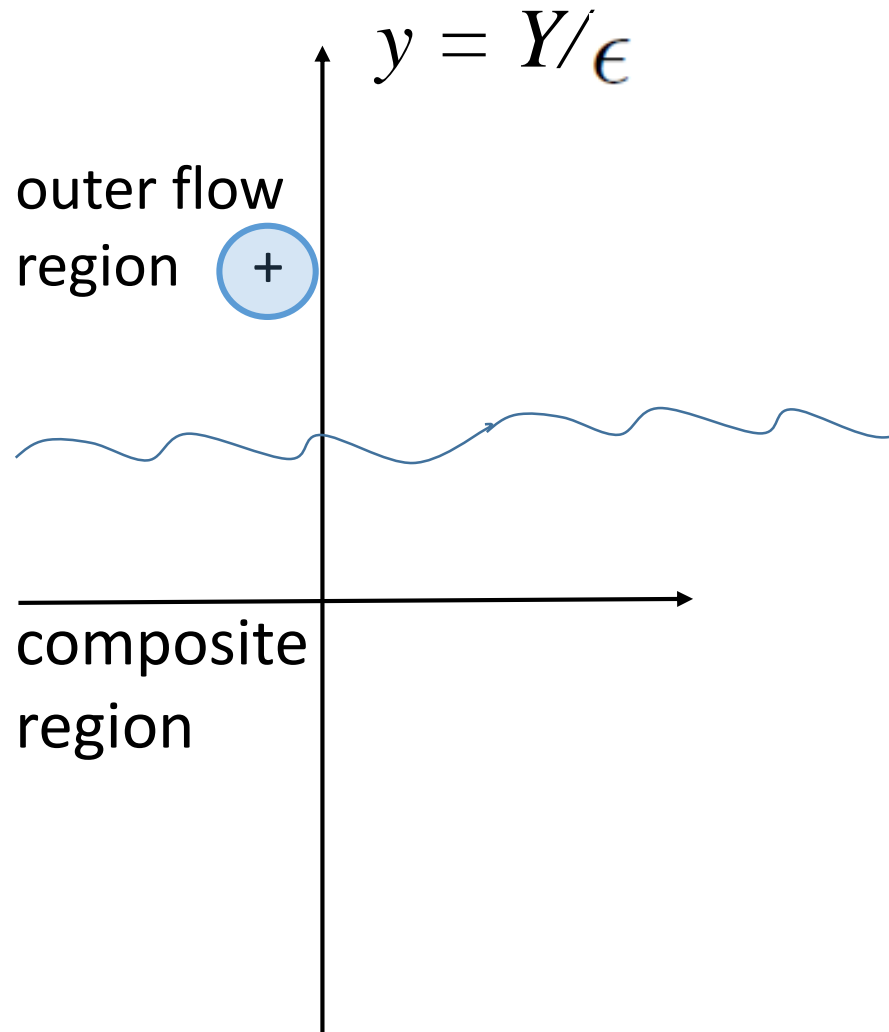


## **BOUNDARY CONDITIONS** (at leading order)

$$\left. \frac{\partial u^{(0)}}{\partial y} \right|_{y \rightarrow +\infty} = S^T, \quad -p^{(0)} \Big|_{y \rightarrow +\infty} = S^N,$$

$$S^T = \frac{\partial U}{\partial Y} + \frac{\partial V}{\partial X} \Big|_{Y \rightarrow 0^+}, \quad S^N = -Re P + 2 \frac{\partial V}{\partial Y} \Big|_{Y \rightarrow 0^+}.$$

1-periodicity for the  $^{(0)}$  fields when  $y \rightarrow -\infty$   
(i.e. in the Darcy region)



## *BOUNDARY CONDITIONS* (at next higher order)

$$\begin{aligned}
 \frac{\partial u^{(1)}}{\partial y} \Big|_{y \rightarrow +\infty} &= - \frac{\partial u^{(0)}}{\partial Y} \Big|_{y \rightarrow +\infty} - \frac{\partial v^{(0)}}{\partial X} \Big|_{y \rightarrow +\infty}, \\
 -p^{(1)} \Big|_{y \rightarrow +\infty} + 2 \frac{\partial v^{(1)}}{\partial y} \Big|_{y \rightarrow +\infty} &= -2 \frac{\partial v^{(0)}}{\partial Y} \Big|_{y \rightarrow +\infty}.
 \end{aligned}$$

1-periodicity for the <sup>(1)</sup> fields when  $y \rightarrow -\infty$



## Microscopic system at leading order:

Homogeneous Stokes equations, plus periodicity in  $x$ , plus forcing from the outer flow

$$\left. \frac{\partial u^{(0)}}{\partial y} \right|_{y \rightarrow +\infty} = S^T, \quad \left. -p^{(0)} \right|_{y \rightarrow +\infty} = S^N,$$

at the edge of the unit cell ( $y = y_\infty$ ), plus 1-periodicity at  $y \rightarrow -\infty$





Linearity permits to express the order zero solution as

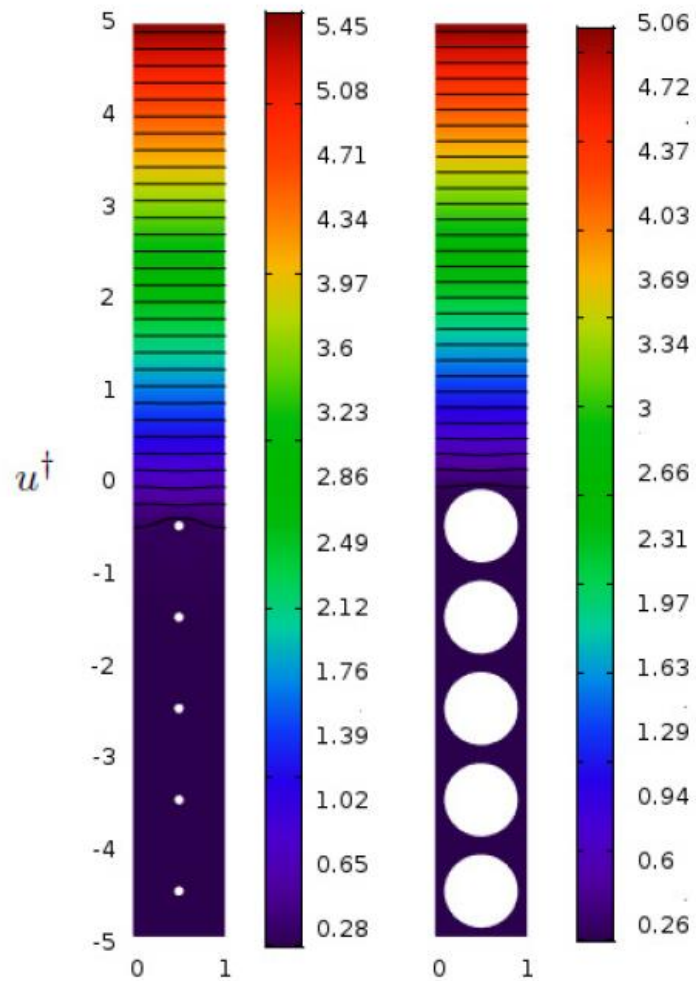
$$u^{(0)} = u^\dagger(x, y) \mathbb{S}^T,$$

$$v^{(0)} = v^\dagger(x, y) \mathbb{S}^T,$$

$$p^{(0)} = p^\dagger(x, y) \mathbb{S}^T - \mathbb{S}^N.$$

so that a Stokes system for the ‘dagger’ variables ensues with

$$\lim_{y \rightarrow +\infty} \frac{\partial u^\dagger}{\partial y} = 1, \quad \lim_{y \rightarrow +\infty} p^\dagger = 0.$$

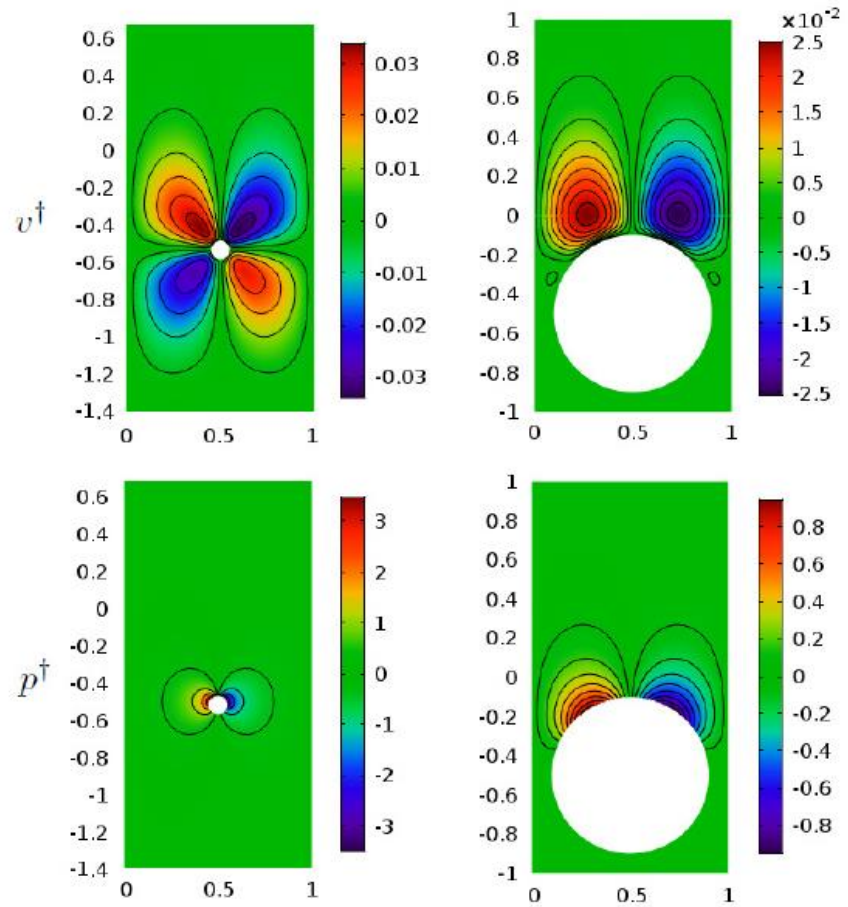


$$u^\dagger|_{y_\infty} = y_\infty + \lambda,$$

$$\theta = 0.4973 \quad \lambda = 1.451 \times 10^{-1}$$

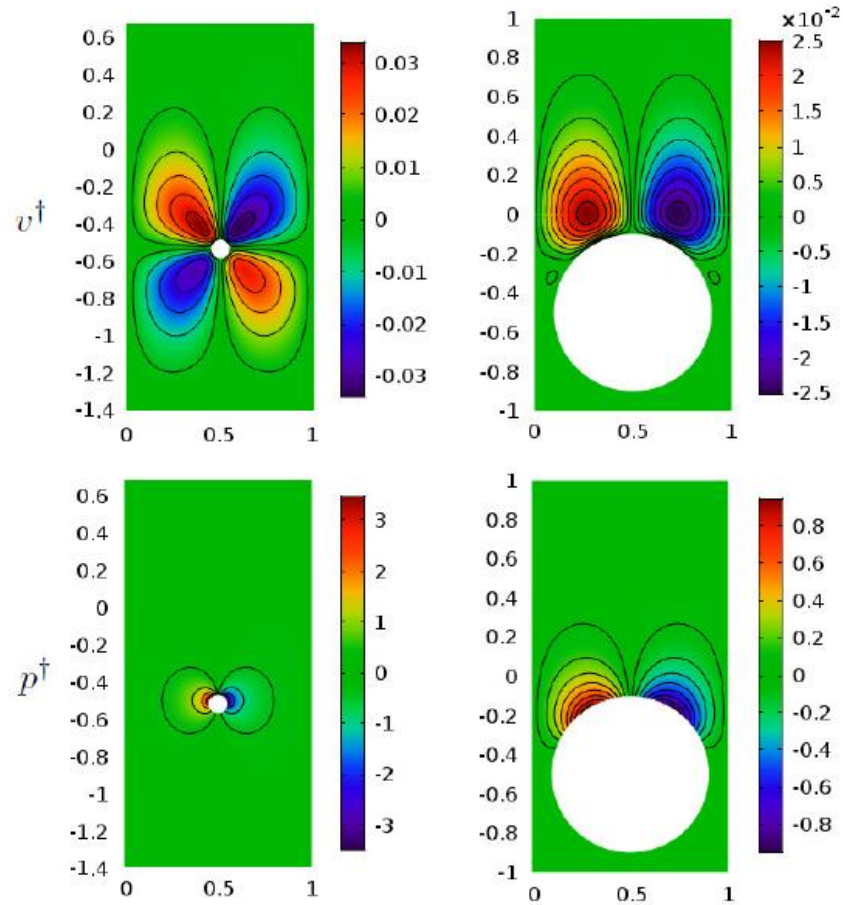
$$\theta = 0.9999 \quad \lambda = 6.188 \times 10^{-1}$$

Fig. 2: Solution of  $u^\dagger$  in the form of isolines for two different porosities,  $\theta = 0.9999$  (left) and  $\theta = 0.4973$  (right) for the case of regularly arranged (also termed *in-line*) two-dimensional solid grains.



$$v^\dagger|_{y_\infty} = 0$$

Fig. 3: Isolines of  $v^\dagger$  (top row) and  $p^\dagger$  (bottom row) for the same conditions as in fig. 2.

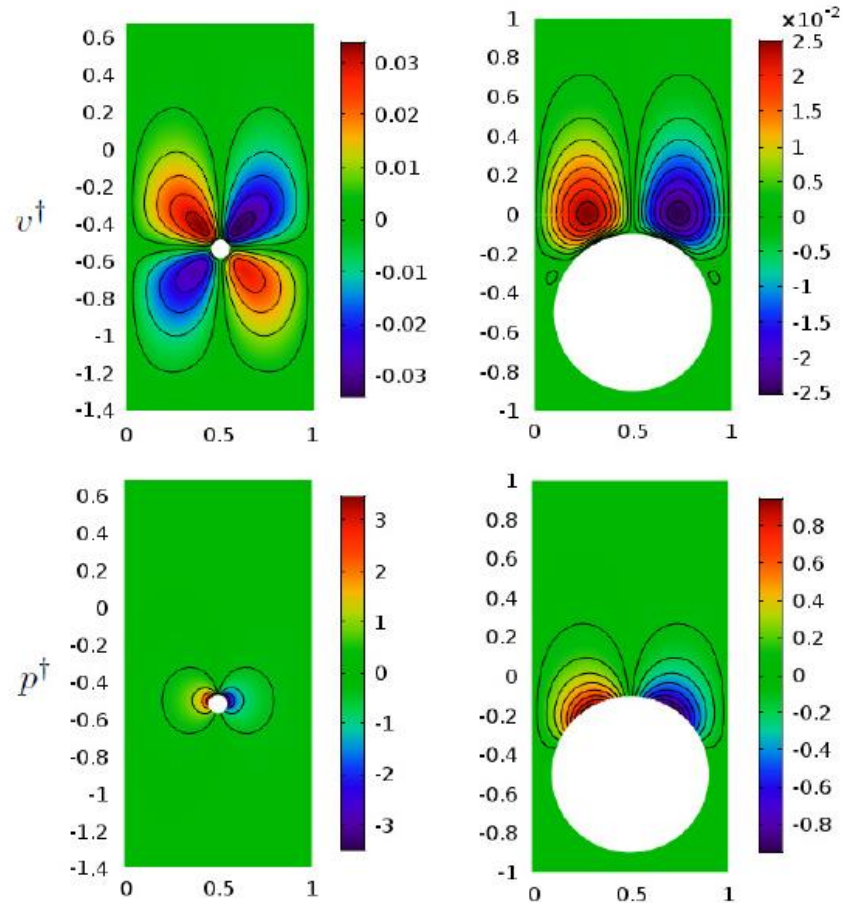


$$v^\dagger|_{y_\infty} = 0$$

$$u_i = u_i^{(0)} + \epsilon u_i^{(1)} + \mathcal{O}(\epsilon^2),$$



$$u|_{y=y_\infty} = (y_\infty + \lambda) S^T + \mathcal{O}(\epsilon), \quad v|_{y=y_\infty} = \mathcal{O}(\epsilon)$$



$$\lim_{y \rightarrow +\infty} (u, v) = \frac{1}{\epsilon} \lim_{Y \rightarrow 0^+} (U, V)$$

$$v^\dagger|_{y_\infty} = 0$$

$$u_i = u_i^{(0)} + \epsilon u_i^{(1)} + \mathcal{O}(\epsilon^2),$$



$$U|_{Y=0^+} = \epsilon \lambda S^T + \mathcal{O}(\epsilon^2), \quad V|_{Y=0^+} = \mathcal{O}(\epsilon^2).$$



## Microscopic system at next order:

$$u_x^{(1)} + v_y^{(1)} = -u_X^{(0)} - v_Y^{(0)},$$

$$-p_x^{(1)} + u_{xx}^{(1)} + u_{yy}^{(1)} = p_X^{(0)} - 2u_{Xx}^{(0)} - 2u_{Yy}^{(0)},$$

$$-p_y^{(1)} + v_{xx}^{(1)} + v_{yy}^{(1)} = p_Y^{(0)} - 2v_{Xx}^{(0)} - 2v_{Yy}^{(0)}.$$

plus boundary conditions:

$$\frac{\partial u^{(1)}}{\partial y} \Big|_{y \rightarrow +\infty} = - \frac{\partial u^{(0)}}{\partial Y} \Big|_{y \rightarrow +\infty} - \frac{\partial v^{(0)}}{\partial X} \Big|_{y \rightarrow +\infty},$$
$$-p^{(1)} \Big|_{y \rightarrow +\infty} + 2 \frac{\partial v^{(1)}}{\partial y} \Big|_{y \rightarrow +\infty} = -2 \frac{\partial v^{(0)}}{\partial Y} \Big|_{y \rightarrow +\infty}.$$



## Microscopic system at next order:

$$\frac{\partial u_i^{(1)}}{\partial x_i} = -u_i^\dagger \frac{\partial S^T}{\partial X_i},$$

$$-\frac{\partial p^{(1)}}{\partial x_i} + \frac{\partial^2 u_i^{(1)}}{\partial x_j^2} = p^\dagger \frac{\partial S^T}{\partial X_i} - \frac{\partial S^N}{\partial X_i} - 2 \frac{\partial u_i^\dagger}{\partial x_j} \frac{\partial S^T}{\partial X_j},$$

plus boundary conditions:

$$\left. \frac{\partial u^{(1)}}{\partial y} \right|_{y \rightarrow \infty} = -u^\dagger \frac{\partial S^T}{\partial Y} - v^\dagger \frac{\partial S^T}{\partial X},$$

$$-p^{(1)} + 2 \left. \frac{\partial v^{(1)}}{\partial y} \right|_{y \rightarrow \infty} = -2 v^\dagger \frac{\partial S^T}{\partial Y}.$$



The solution has the form:

$$u_i^{(1)} = \tilde{u}_{ij} \frac{\partial S^T}{\partial X_j} + \check{u}_{ij} \frac{\partial S^N}{\partial X_j}$$

$$p^{(1)} = \tilde{p}_j \frac{\partial S^T}{\partial X_j} + \check{p}_j \frac{\partial S^N}{\partial X_j},$$



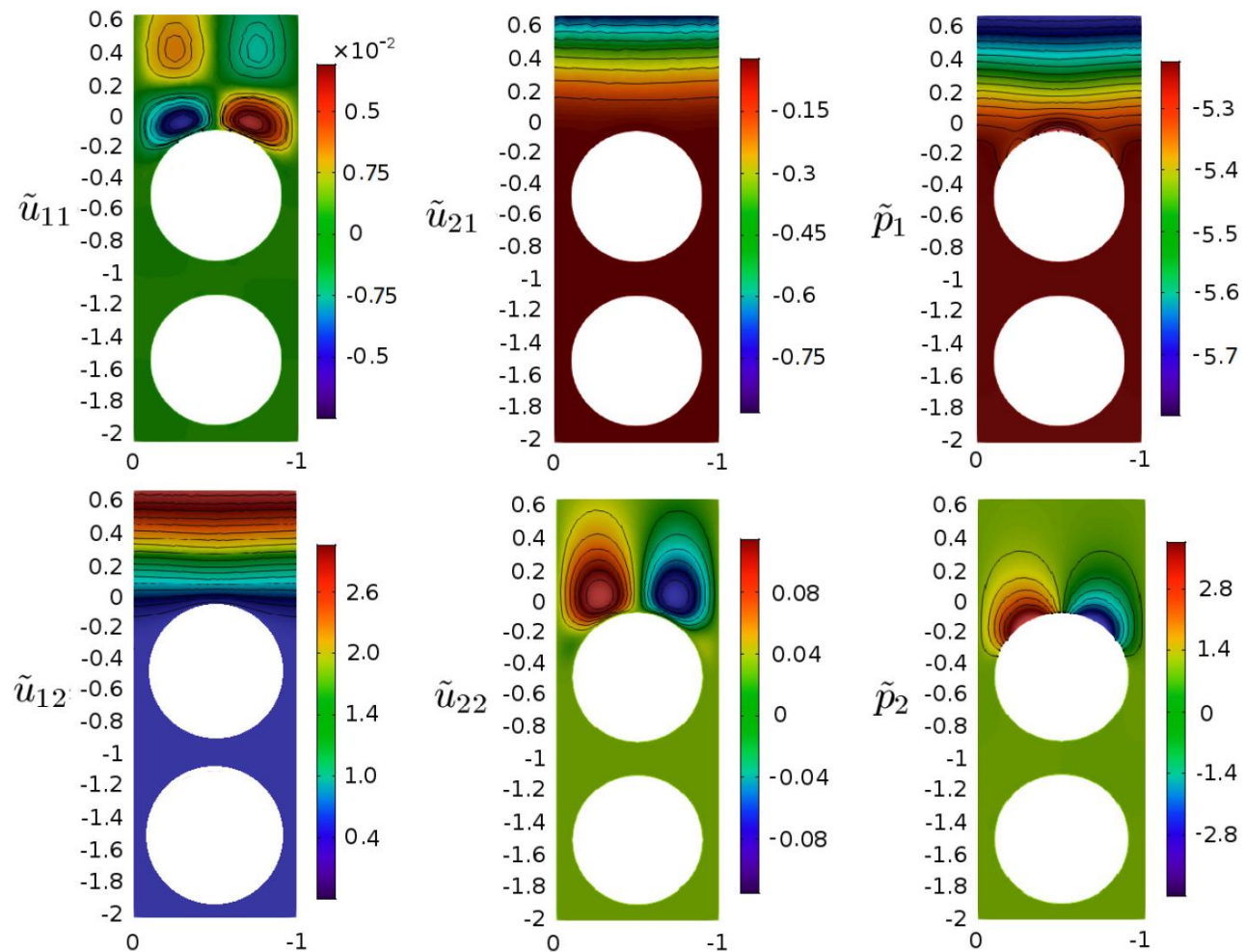


Fig. 4: Fields of  $\tilde{u}_{ij}$  and  $\tilde{p}_j$  in the neighborhood of the dividing surface for regularly arranged two-dimensional solid grains, porosity  $\theta = 0.4973$ .

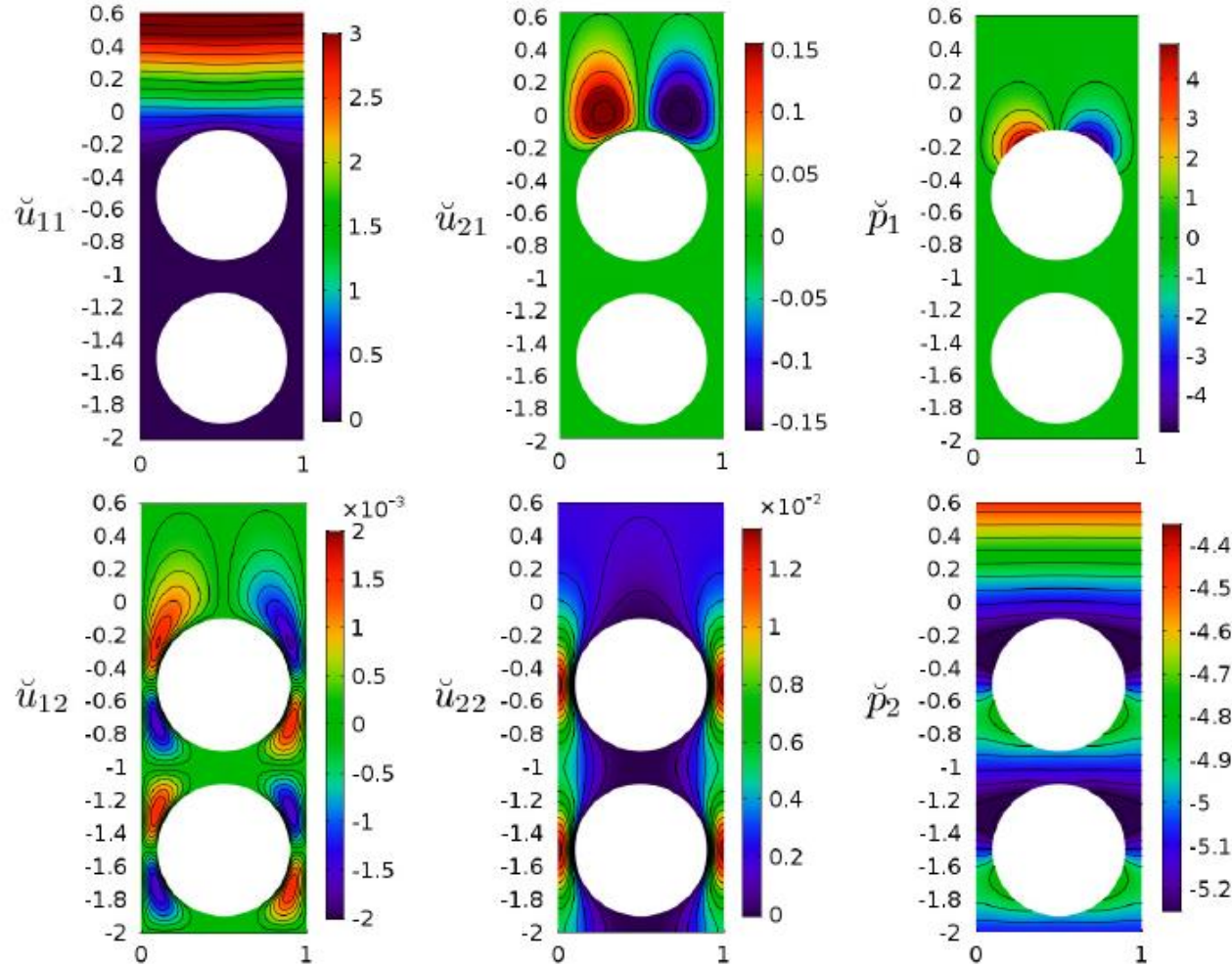


Fig. 5: Same as figure 4 for  $\check{u}_{ij}$  and  $\check{p}_j$ .

$$-\tilde{u}_{21}|_{y_\infty} = \check{u}_{11}|_{y_\infty} = \frac{y_\infty^2}{2} + \lambda y_\infty + \mathcal{K}^{itf}$$

$$\check{u}_{22}|_{y_\infty} = \mathcal{K}$$



$$u_i^{(1)} = \tilde{u}_{ij} \frac{\partial S^T}{\partial X_j} + \check{u}_{ij} \frac{\partial S^N}{\partial X_j}$$

The **macroscopic** effective conditions at  $Y=0^+$  are:

$$U|_{Y=0^+} = \epsilon \lambda S^T \Big|_{Y=0^+} + \epsilon^2 \mathcal{K}^{itf} \frac{\partial S^N}{\partial X} \Big|_{Y=0^+} + \mathcal{O}(\epsilon^3),$$

$$V|_{Y=0^+} = -\epsilon^2 \mathcal{K}^{itf} \frac{\partial S^T}{\partial X} \Big|_{Y=0^+} + \epsilon^2 \mathcal{K} \frac{\partial S^N}{\partial Y} \Big|_{Y=0^+} + \mathcal{O}(\epsilon^3).$$



For the case of a regularly microstructured rough solid wall we had previously found:

$$U(X, 0, t) = \epsilon \lambda_x S^T + \epsilon^2 m_{12} S_X^N + \mathcal{O}(\epsilon^3)$$

$$V(X, 0, t) = \epsilon^2 m_{21} S_X^T + \mathcal{O}(\epsilon^3)$$

with  $S^T = U_Y + V_X$ ,  $S^N = -ReP + 2V_Y$ , evaluated at  $Y = 0$

(Bottaro & Naqvi, *Meccanica*, Vol. 55, 2020)

## 2D

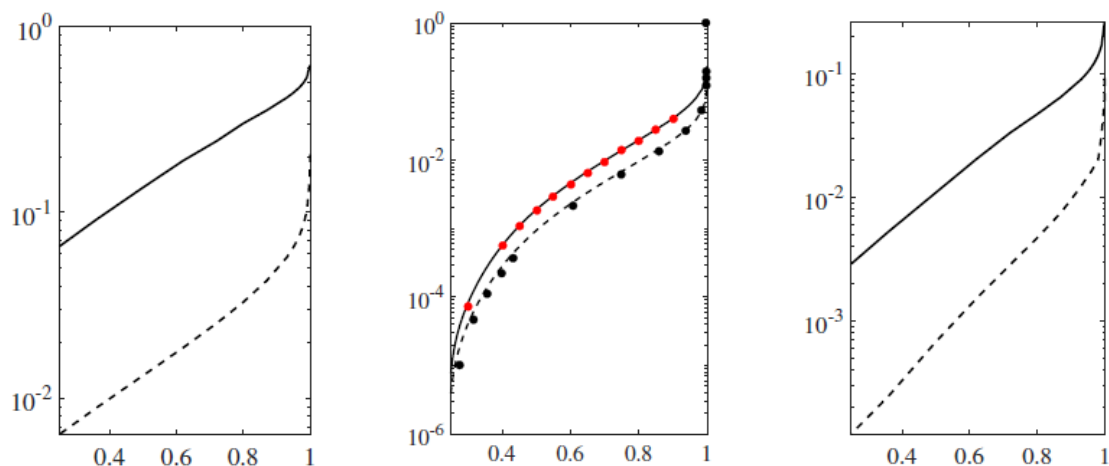


Fig. 6: Comparison between regularly arranged grains (solid lines) and staggered grains (dashed lines) for two-dimensional isotropic porous media of varying porosity  $\theta$  (plotted in abscissa in all frames). From left to right:  $\lambda$ ,  $\mathcal{K}$  and  $\mathcal{K}^{itf}$ . In the central frame the medium permeabilities for in-line and staggered cases are validated, respectively, against [31] (red circles) and [5] (black circles).

## 3D

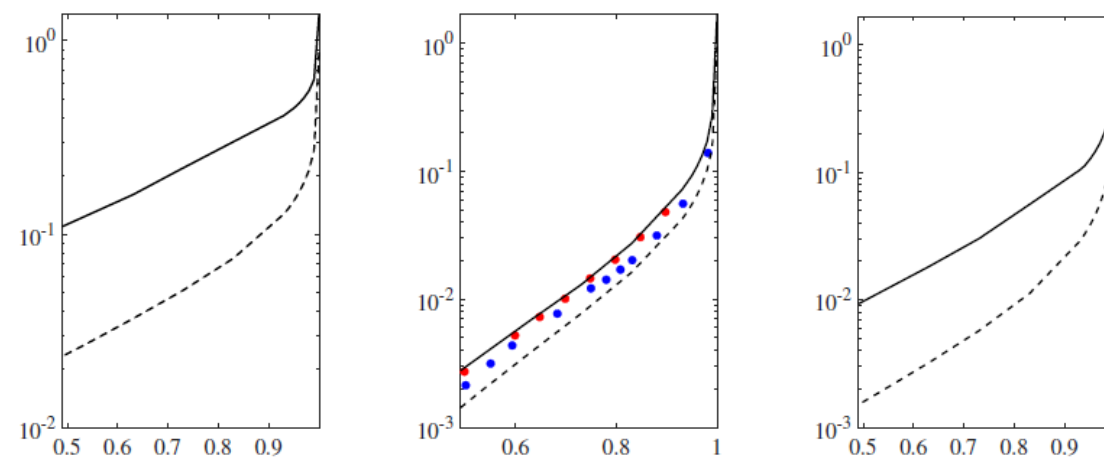


Fig. 7: Same as figure 6 for three-dimensional spherical grains. In the central frame the permeability for the in-line arrangement of spheres is compared to results in [31] (red circles). The permeability results for Wigner-Seitz grains [20] are given with blue circles.



Our condition is different from Saffman's ... it does not couple the inner (Darcy) flow to the outer flow, except via the coefficients (which depend on pore geometry).



Our condition is different from Saffman's ... it does not couple the inner (Darcy) flow to the outer flow, except via the coefficients (which depend on pore geometry).

What about the pore pressure?



$$\langle a \rangle^f := \frac{1}{\mathcal{V}_{fluid}} \int_{\mathcal{V}_{fluid}} a \, dV$$

The pressure is:

$$p = p^\dagger S^T - S^N + \epsilon \tilde{p}_j \frac{\partial S^T}{\partial X_j} + \epsilon \check{p}_j \frac{\partial S^N}{\partial X_j} + \mathcal{O}(\epsilon^2).$$





$$\langle a \rangle^f := \frac{1}{\mathcal{V}_{fluid}} \int_{\mathcal{V}_{fluid}} a \, dV$$

The pressure is:

$$p = p^\dagger S^T - S^N + \epsilon \tilde{p}_j \frac{\partial S^T}{\partial X_j} + \epsilon \check{p}_j \frac{\partial S^N}{\partial X_j} + \mathcal{O}(\epsilon^2).$$

so that

$$\langle p \rangle_{-\infty}^f = -S^N + \epsilon \langle \tilde{p}_1 \rangle_{-\infty}^f \frac{\partial S^T}{\partial X} + \epsilon \langle \check{p}_2 \rangle_{-\infty}^f \frac{\partial S^N}{\partial Y} + \mathcal{O}(\epsilon^2).$$

with the phase averaged pressure in the porous (i.e. - ) domain defined by:

$$\langle p \rangle_{-\infty}^f = P_0^- |_{Y=0^-} + \epsilon \langle P_1^- \rangle_{-\infty}^f + \mathcal{O}(\epsilon^2),$$



Thus:

$$P_0^- |_{Y=0^-} = -S_N + \mathcal{O}(\epsilon)$$




$$U |_{Y=0^+} = \epsilon \lambda S^T |_{Y=0^+} - \epsilon^2 \mathcal{K}^{itf} \frac{\partial P_0^-}{\partial X} |_{Y=0^-} + \mathcal{O}(\epsilon^3).$$

Furthermore, mass conservation and x-periodicity yield:

$$V |_{Y=0^+} = -\epsilon^2 \mathcal{K} \frac{\partial P_0^-}{\partial Y} |_{Y=0^-} + \mathcal{O}(\epsilon^3).$$



Saffman's condition is indeed valid   
and the coefficients are available through the  
solution of two simple Stokes problems.

$$U|_{Y=0^+} = \epsilon \lambda S^T \Big|_{Y=0^+} - \epsilon^2 \mathcal{K}^{itf} \frac{\partial P_0^-}{\partial X} \Big|_{Y=0^-} + \mathcal{O}(\epsilon^3).$$

$$V|_{Y=0^+} = -\epsilon^2 \mathcal{K} \frac{\partial P_0^-}{\partial Y} \Big|_{Y=0^-} + \mathcal{O}(\epsilon^3).$$

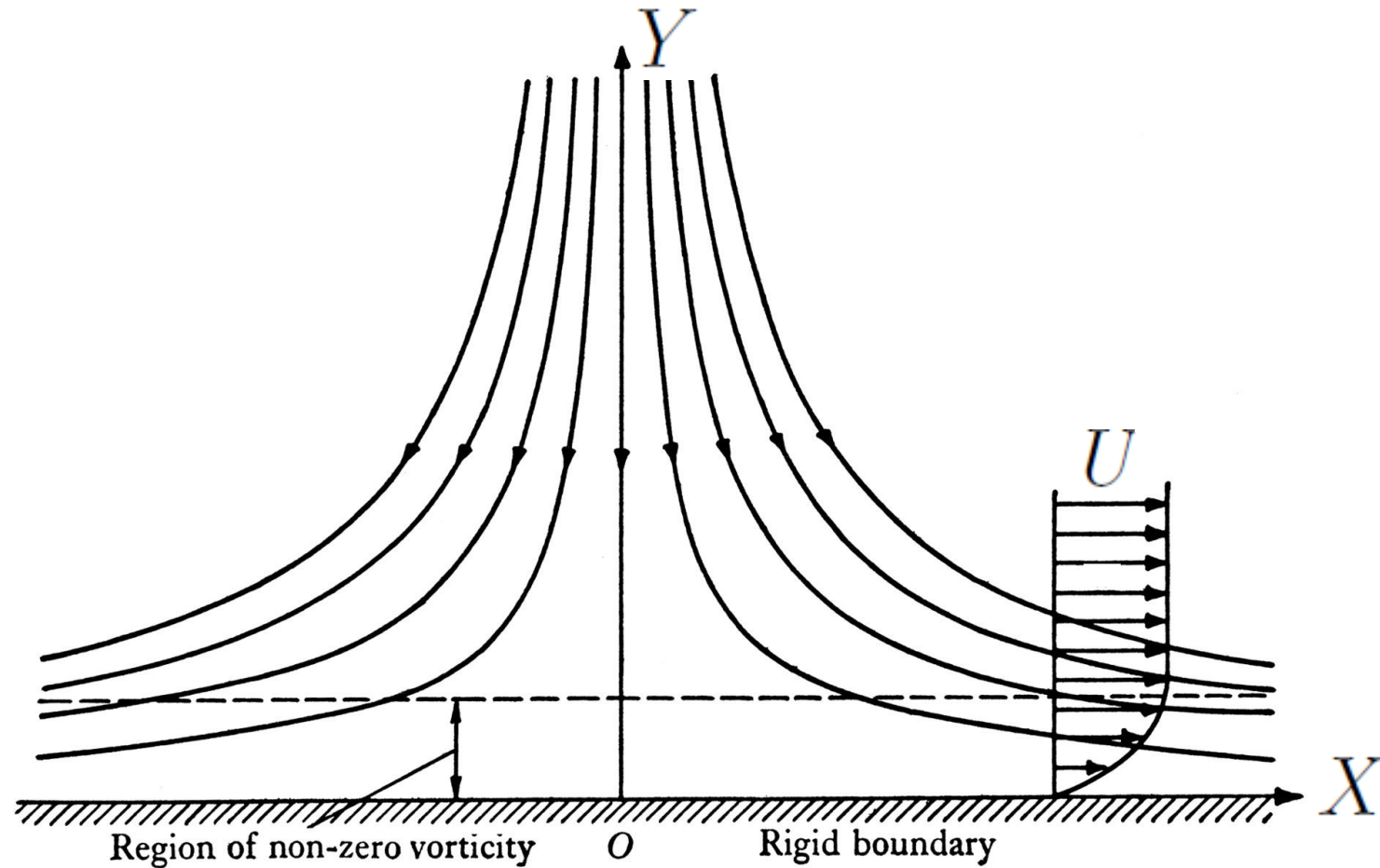


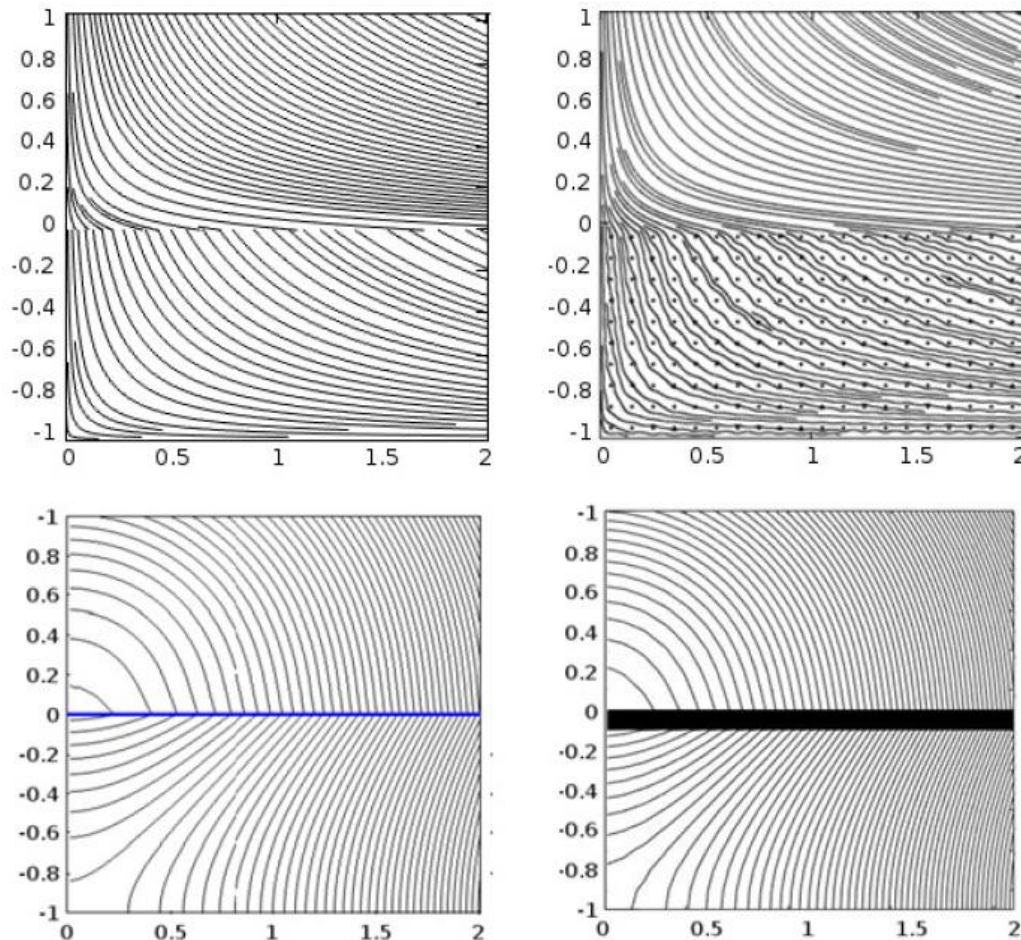
## Macroscopic tests of the conditions at the dividing surface

1. Hiemenz flow over a porous wall
2. Backward facing (porous) step



## Macroscopic test 1: the Hiemenz stagnation point flow





**Significant infiltration of fluid within a porous medium of very large porosity.**

In the porous region the solution is found, in the model case, simply by forcing the pressure to be a harmonic function with a Dirichlet condition on  $Y = 0^-$ .

The feature-resolving simulation captures the flow through the pores via solution of the Navier-Stokes equations through the whole domain.

$(\epsilon = 0.1)$

Fig. 8: Streamlines (top row) and pressure contours (bottom row) close to the axes' origin, both in the free-fluid and the porous region. The frames on the left correspond to solutions obtained with the two-domain approach; results on the right are obtained by fully resolving the flow, also through the solid inclusions. The pressure in the bottom right frame is the intrinsic averaged pressure.

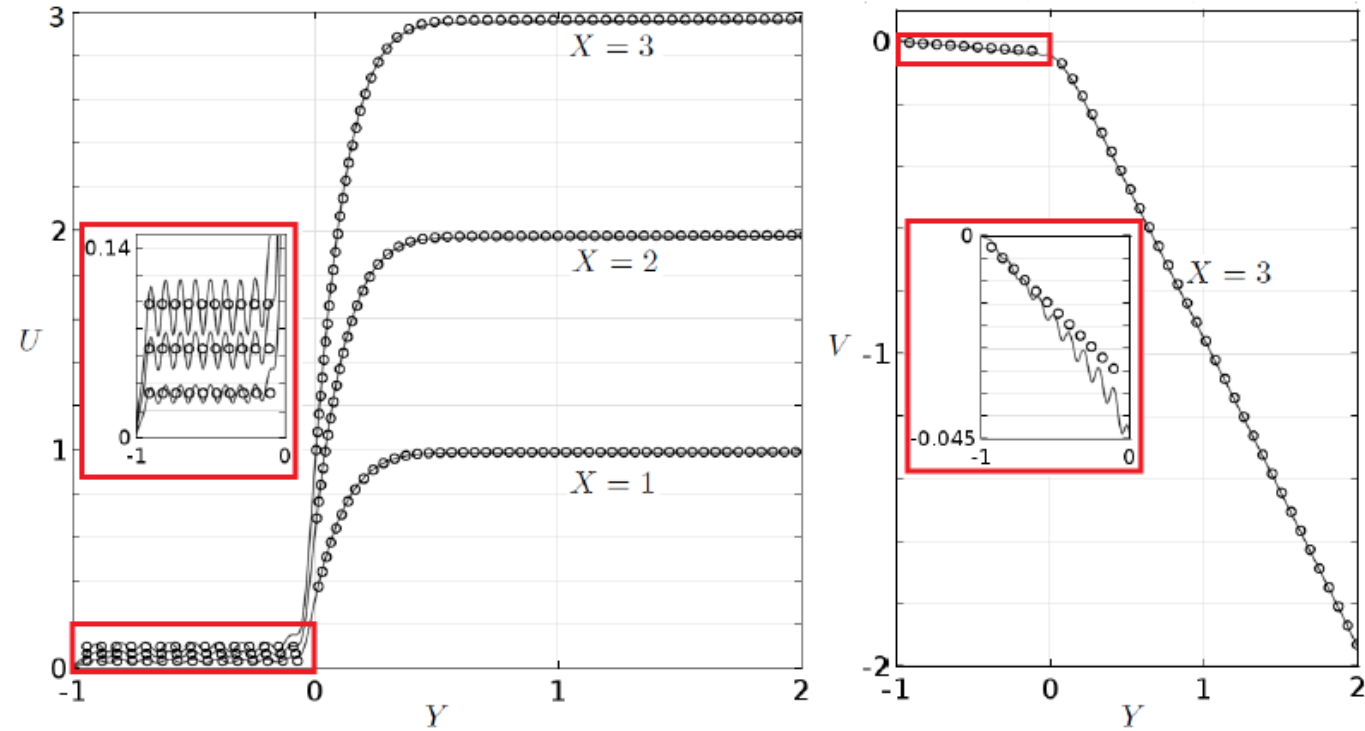
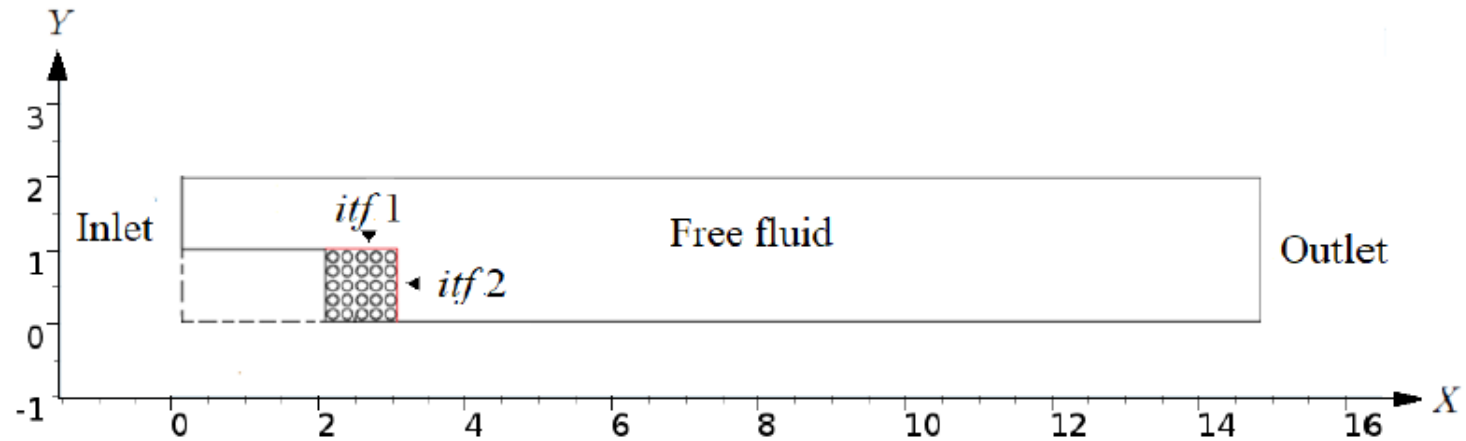


Fig. 9: Comparison between complete simulation with full feature resolution (solid lines) and modeled with slip/transpiration velocity imposed at the dividing line (empty circles). Longitudinal velocity component  $U$  (left) and normal velocity component  $V$  (right) as a function of  $Y$ . The insets highlight the velocity distributions in the porous domain.



## Macroscopic test 2: the backward-facing step





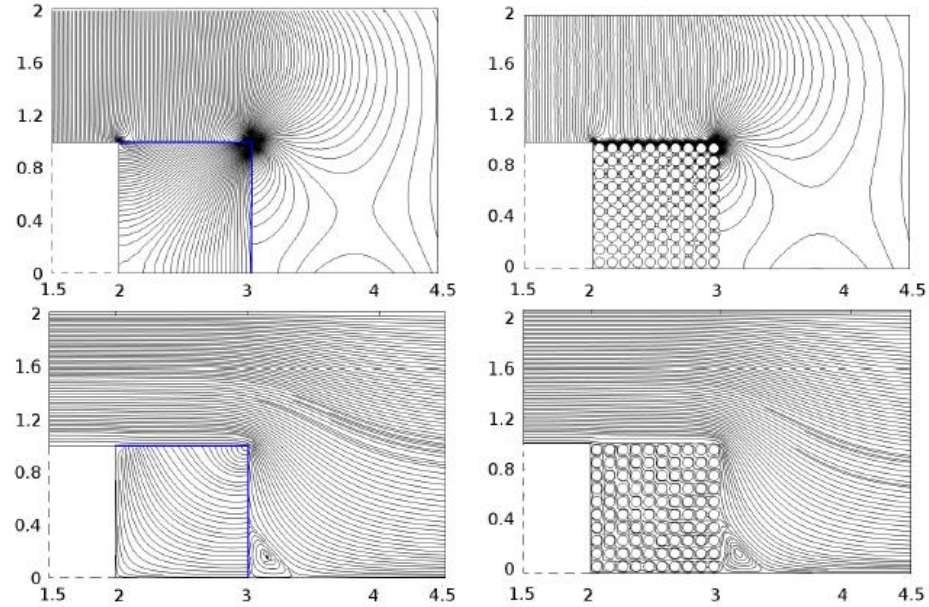


Fig. 11: Comparison between the solutions for  $Re = 0.0001$  of the two-domain approach (left frames, with blue lines denoting the dividing surfaces) and the *exact* feature-resolving numerical solution of the equations, also through the pores (right frames), focussing around the neighborhood of the step. The top row of images displays the pointwise pressure contours; streamlines are plotted in the bottom row.

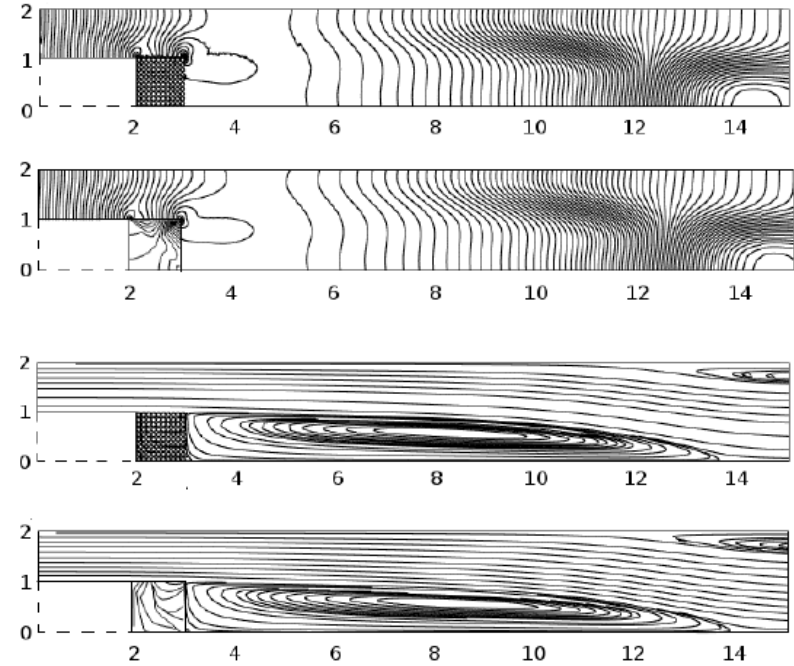


Fig. 12: Same quantities as in figure 11, plotted in the whole domain ( $Re = 500$ ).

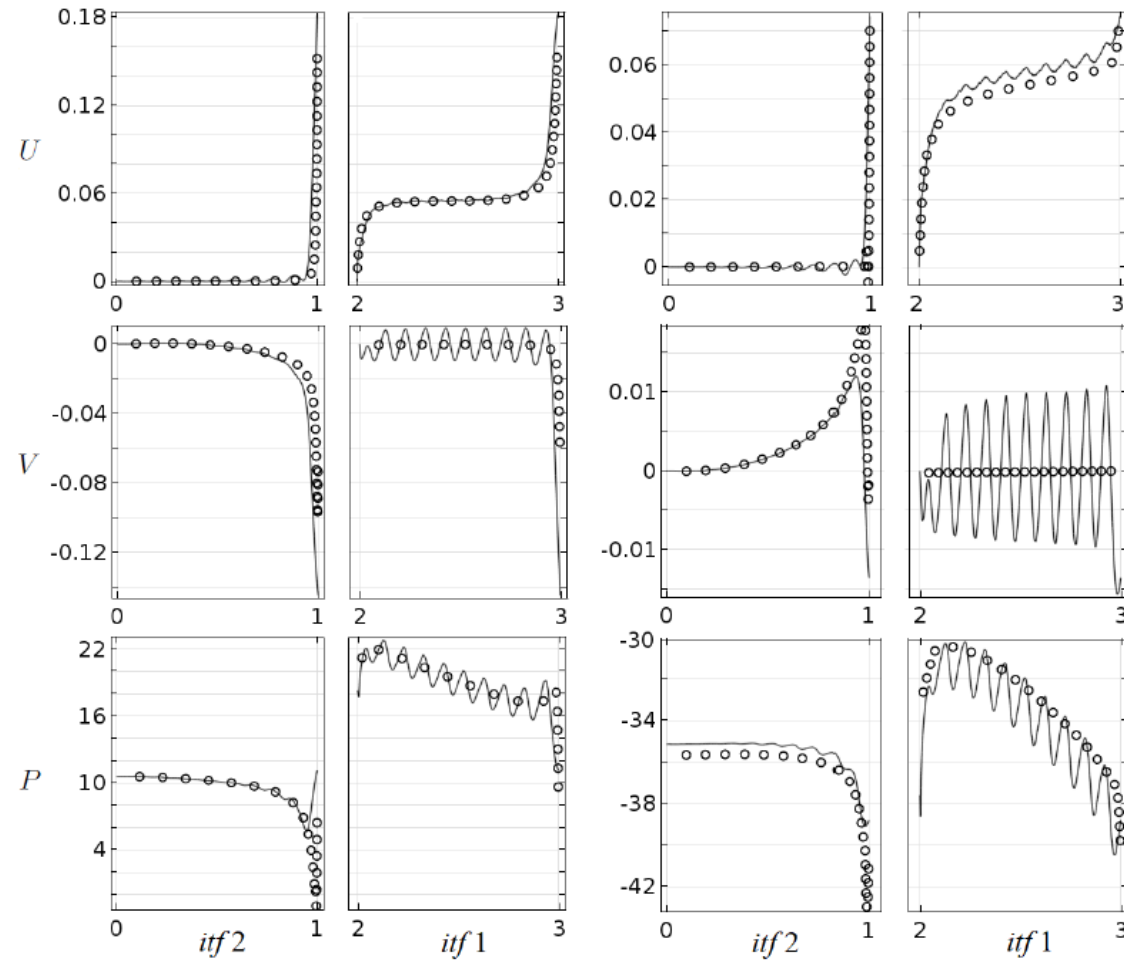


Fig. 13: Comparison of velocity components  $U$ ,  $V$  and pressure  $P$  for  $Re = 0.0001$  (six frames on the left) and  $Re = 500$  (six frames on the right), for the two interfaces. The feature-resolving solutions are shown with solid lines and results of the two-domain approach are displayed with symbols.



## Summary

1. We have developed second order conditions to be employed at the dividing surface between a free-fluid region and a porous, regularly micro-structured, medium. Conditions are given in **two equivalent forms**: one coincides with a little-noticed extension of Saffman's result, the second is new and does not require iterations between the free-fluid and the porous solvers. Both formulations require knowledge of three coefficients, a **permeability coefficient** (a tensor for the case of anisotropic porous media), an **interface permeability coefficient** (tensor) and a **Navier-slip coefficient** (tensor), available via solutions of auxiliary, microscopic Stokes-like problems in elongated unit cells.



## Summary (continued)

2. Conditions are formally correct for  $\epsilon \rightarrow 0$ , but macroscopic results seem to be acceptable for rather large values of  $\epsilon$
3. Conditions work well also for reasonably large values of the outer Reynolds number
4. Simple extension to anisotropic porous media in 3D



## Future developments (SHS/LIS):

1. include a lubricant fluid within the pores (VOF in unit cell)
2. perform DNS with slip/transpiration for turbulent channel flow over a porous layer (first) and a LIS (later) and compare to feature-resolving DNS
3. optimise morphology of porous material, impregnated with lubricant, and optimise properties of lubricant fluid